Parallel Solution of Dynamic Elasticity Problems

Ivan Dyyak(✉), Vitaliy Horlatch, and Marianna Salamakha

Ivan Franko National University of Lviv, 1 Universytetska St., Lviv 79000, Ukraine
Ivan.dyyak@lnu.edu.ua

Abstract. An algorithm for parallel solution of the dynamic problems of the elasticity theory for axisymmetric objects as a three-dimensional problem of the elasticity theory has been proposed. The semidiscrete approximations reduce the problem to the solution of the Cauchy problem for a system of linear differential equations of the second order. The elements of the matrix are determined with the help of the semi-analytical finite element method (FEM) using the Fourier series analytical expansion by trigonometric functions of the angle coordinate and numerical expansion of isoparametric approximations on serendipity quadrilaterals in the meridional section. The Cauchy problem is solved by decomposing the solution into eigenfunctions, which we find using the subspace iterations method. The method has been parallelized with domain decomposition and message passing interface (MPI), and the parallelized method has been scaled to over 20 processors with high parallel performance. The numerical examples have demonstrated the performance of the proposed algorithm. The numerical results indicate that the method is very accurate and its parallelizations are efficient for both types of problems.

Keywords: Axisymmetric anisotropic objects · Dynamic elasticity · Finite element method · The eigenvalue problem · The algorithm of parallelization

1 Introduction

A detailed study on the dynamic behavior of various elements of engineering structures is widely possible using modern numerical methods. It has been used in areas such as geological surveys, sound reduction, crack detection or even in earthquake propagation studies. Although 3D finite elements are universal and can be used to solve dynamic problems for structures of various complex geometry, they need huge computing capacity. The aim of this paper is to design an algorithm by combining several well-established mathematical methods with some new approaches for the efficient solution of dynamic problems for axisymmetric structures in a way involving less computational cost. Different structures of cylindrical shape elements are very often used as parts of important engineering constructions. For this reason, dynamic behavior of such structures has been extensively investigated in recent years. FEM in the form of the semidiscrete Galerkin method is so far the currently dominating one for dynamic

© Springer Nature Switzerland AG 2020
V. Ivanov et al. (Eds.): DSMIE 2019, LNME, pp. 562–571, 2020.
https://doi.org/10.1007/978-3-030-22365-6_56

analysis of such objects. The use of the eigenfunction expansion method for time integration together with semi-analytical FEM has become a good basis for the algorithms of parallelization [1].

2 Literature Review

Currently, there is renewed interest in this area due to advances in the development of ultrasonic and microsonic based devices for trapping of biological cells and micro particles [2]. Two types of dynamic problems are usually considered: dynamic response of a structure sustaining arbitrary loading [3, 4] and free vibration [5, 6]. As noted in [7], despite the significant growth in the breadth of its applicability, two areas have received relatively less attention in p/hp-FEM for solid mechanics: dynamic problems and parallelism [8]. A Chebyshev-Ritz numerical procedure based on the 3D elasticity theory is employed in [5] to extract the full vibration spectrum of natural frequencies along with selected 3D deformed mode shapes. To study a number of problems of harmonic and impulse oscillations, an approach of fundamental solutions for layers was developed on the basis of which amplitude characteristics, as well as stress diagrams for layers with one or two cavities of different types, were obtained [9]. Paper [3] presents an explicit smoothed finite element method (SFEM) for elastic dynamic problems. The central difference method for time integration is used in presented formulations. A spectral method for elastic wave calculations which is based on a Chebychev expansion in the vertical direction is presented in [4]. The results indicate that the method presents an improvement over the ordinary Fourier method in handling the free surface boundary condition. An algorithm that is able to solve dynamic contact problems with complex local geometries was proposed in [10]. The authors combined domain decomposition with mortar coupling, contact modeling via semismooth Newton methods and energy-consistent time integration. Numerical examples confirm the optimality of the approach and its stabilization effect applied to dynamic contact problems.

3 Research Methodology

3.1 Governing Equations

Let us consider the deformation of a three-dimensional object that occupies the axisymmetric domain of an anisotropic, linearly elastic material. The domain is referred to a right-hand system of orthogonal, cylindrical coordinates r, θ and z which represent the radial, angular and axial coordinates, respectively.

The dynamic problem of elasticity is investigated in a 3D statement. The independent displacement components that describe the motion of the body can be written as

$$u_r \equiv u_r(r,\theta,z,t), \quad u_\theta \equiv u_\theta(r,\theta,z,t), \quad u_z \equiv u_z(r,\theta,z,t), \quad \mathbf{u} \equiv (u_r, u_\theta, u_z)^T, \quad (1)$$

The equations of motion corresponding to the displacement field (1) can be expressed as [6]:

$$\begin{aligned}
&\frac{\partial \sigma_{rr}}{\partial r}+\frac{1}{r}\frac{\partial \sigma_{r\theta}}{\partial \theta}+\frac{\partial \sigma_{rz}}{\partial z}+\frac{\sigma_{rr}-\sigma_{\theta\theta}}{r}=\rho\frac{\partial^2 u_r}{\partial t^2},\\
&\frac{\partial \sigma_{r\theta}}{\partial r}+\frac{1}{r}\frac{\partial \sigma_{\theta\theta}}{\partial \theta}+\frac{\partial \sigma_{\theta z}}{\partial z}+\frac{2\sigma_{r\theta}}{r}=\rho\frac{\partial^2 u_\theta}{\partial t^2},\\
&\frac{\partial \sigma_{rz}}{\partial r}+\frac{1}{r}\frac{\partial \sigma_{\theta z}}{\partial \theta}+\frac{\partial \sigma_{zz}}{\partial z}+\frac{\sigma_{rz}}{r}=\rho\frac{\partial^2 u_z}{\partial t^2}
\end{aligned} \tag{2}$$

Here ρ is the density of the material. We also assume that the relations for strain components and constitutive relations are given in matrix form as

$$\boldsymbol{\varepsilon}\equiv\begin{Bmatrix}\varepsilon_{rr}\\ \varepsilon_{\theta\theta}\\ \varepsilon_{zz}\\ \varepsilon_{rz}\\ \varepsilon_{r\theta}\\ \varepsilon_{z\theta}\end{Bmatrix}=\begin{bmatrix}\frac{\partial}{\partial r} & 0 & 0\\ \frac{1}{r} & \frac{1}{r}\frac{\partial}{\partial\theta} & 0\\ 0 & 0 & \frac{\partial}{\partial z}\\ \frac{1}{2}\frac{\partial}{\partial z} & 0 & \frac{1}{2}\frac{\partial}{\partial r}\\ \frac{1}{2r}\frac{\partial}{\partial\theta} & \frac{\partial}{\partial r}-\frac{1}{r} & 0\\ 0 & \frac{1}{2}\frac{\partial}{\partial z} & \frac{1}{2r}\frac{\partial}{\partial\theta}\end{bmatrix}\cdot\begin{Bmatrix}u_r\\ u_\theta\\ u_z\end{Bmatrix}, \tag{3}$$

and

$$\boldsymbol{\sigma}\equiv\begin{Bmatrix}\sigma_{rr}\\ \sigma_{\theta\theta}\\ \sigma_{zz}\\ \sigma_{rz}\\ \sigma_{r\theta}\\ \sigma_{z\theta}\end{Bmatrix}=\begin{bmatrix}d_{11} & d_{12} & d_{13} & 0 & 0 & 0\\ d_{12} & d_{22} & d_{23} & 0 & 0 & 0\\ d_{31} & d_{32} & d_{33} & 0 & 0 & 0\\ 0 & 0 & 0 & d_{44} & 0 & 0\\ 0 & 0 & 0 & 0 & d_{55} & 0\\ 0 & 0 & 0 & 0 & 0 & d_{66}\end{bmatrix}\cdot\begin{Bmatrix}\varepsilon_{rr}\\ \varepsilon_{\theta\theta}\\ \varepsilon_{zz}\\ \varepsilon_{rz}\\ \varepsilon_{r\theta}\\ \varepsilon_{z\theta}\end{Bmatrix}, \tag{4}$$

respectively. The constitutive relations (4) contain nine independent elastic constants and involve the most widely used kinds of anisotropic media: transversely isotropic and orthotropic.

There are external loads applied to the surface of the object

$$\sum_{i,j}^{3}\sigma_{ij}n_j=\zeta_i,\quad \mathrm{i,j}=\mathrm{r},\theta,\mathrm{z},\quad \text{on}\quad \Gamma_N. \tag{5}$$

here Γ_N is the part of the surface of the cylinder, n_r, n_θ, n_z are the components of the outward unit normal vector to this surface in radial, angular and axial directions respectively, and $\zeta_i(i=r,\theta,z)$—are prescribed loads. Moreover, we also have the kinematic boundary conditions

$$\mathbf{u}=\mathbf{g},\quad \text{on}\ \Gamma_D,\quad \Gamma\equiv\partial\Omega=\Gamma_N\cup\Gamma_D,\quad \Gamma_N\cap\Gamma_D=\varnothing, \tag{6}$$

where $\boldsymbol{g} = (g_r, g_\theta, g_z)^T$ is the given vector of displacements and initial conditions:

$$\mathbf{u}|_{t=0} = \mathbf{0}, \quad \frac{\partial \mathbf{u}}{\partial t}|_{t=0} = \mathbf{0}, \quad x \in \Omega. \tag{7}$$

$\boldsymbol{\varepsilon} \equiv \left(\varepsilon_{rr}, \varepsilon_{zz}, \varepsilon_{\theta\theta}, \varepsilon_{rz,}\varepsilon_{r\theta}, \varepsilon_{\theta z}\right)^T$—is the vector of the deformations component in (3), and $\boldsymbol{\sigma} \equiv \left(\sigma_{rr}, \sigma_{zz}, \sigma_{\theta\theta}, \sigma_{rz,}\sigma_{r\theta}, \sigma_{\theta z}\right)^T$—is the vector of the stresses component in (4).

3.2 Weak Formulation

Let us introduce the space of kinematically admissible vectors of displacement, which is analogous to [6]

$$V = \left\{ \mathbf{v} = \left(v_r, v_\theta, v_z\right)^T : \quad v_i = 0 \quad \text{на} \;\; \Gamma_D, \quad v_i \in H^1(\Omega), \quad i = r, \theta, z \right\}.$$

The weak variational form of the initial-boundary problem (2), (5)–(7) is formulated as:

Find $\mathbf{u} \in H$ such that

$$\begin{aligned} &m(\mathbf{u}''(t), \mathbf{v}) + a(\mathbf{u}(t), \mathbf{v}) = \langle l(t), \mathbf{v} \rangle, \quad \forall \mathbf{v} \in V, \quad \forall t \in (0; T], \\ &\mathbf{u}(0) = \mathbf{0}, \quad \mathbf{u}'(0) = \mathbf{0}. \end{aligned} \tag{8}$$

where bilinear forms:

$$m(\mathbf{u}, \mathbf{v}) = \int_\Omega \rho(u_r v_r + u_\theta v_\theta + u_z v_z) d\Omega,$$

and

$$\begin{aligned} a(\mathbf{u}, \mathbf{v}) = \int_\Omega \Bigg\{ & d_{11} \frac{\partial u_r}{\partial r} \frac{\partial v_r}{\partial r} + d_{12} \left(\frac{\partial u_z}{\partial z} \frac{\partial v_r}{\partial r} + \frac{\partial u_r}{\partial r} \frac{\partial v_z}{\partial z} \right) \\ & + \frac{d_{13}}{r} \left(u_r \frac{\partial v_r}{\partial r} + v_r \frac{\partial u_r}{\partial r} + \frac{\partial u_\theta}{\partial \theta} \frac{\partial v_r}{\partial r} + \frac{\partial u_r}{\partial r} \frac{\partial v_\theta}{\partial \theta} \right) + d_{22} \frac{\partial u_z}{\partial z} \frac{\partial v_z}{\partial z} \\ & + \frac{d_{23}}{r} \left(\frac{\partial u_z}{\partial z} v_r + \frac{\partial v_z}{\partial z} u_r + \frac{\partial u_z}{\partial z} \frac{\partial v_\theta}{\partial \theta} + \frac{\partial v_z}{\partial z} \frac{\partial u_\theta}{\partial \theta} \right) + \frac{d_{33}}{r^2} (u_r v_r \\ & + \frac{\partial u_\theta}{\partial \theta} \frac{\partial v_\theta}{\partial \theta} + \frac{\partial u_\theta}{\partial \theta} v_r + \frac{\partial v_\theta}{\partial \theta} u_r \Bigg) + d_{44} \left(\frac{\partial u_r}{\partial z} \frac{\partial v_r}{\partial z} + \frac{\partial u_z}{\partial r} \frac{\partial v_z}{\partial r} \right. \\ & \left. + \frac{\partial u_z}{\partial r} \frac{\partial v_r}{\partial z} + \frac{\partial u_r}{\partial z} \frac{\partial v_z}{\partial r} \right) + d_{55} \left(\frac{1}{r} \frac{\partial v_r}{\partial \theta} \left(\frac{\partial u_\theta}{\partial r} - \frac{u_\theta}{r} \right) \right. \\ & \left. + \frac{1}{r} \frac{\partial u_r}{\partial \theta} \left(\frac{\partial v_\theta}{\partial r} - \frac{v_\theta}{r} \right) + \left(\frac{\partial u_\theta}{\partial r} - \frac{u_\theta}{r} \right) \left(\frac{\partial v_\theta}{\partial r} - \frac{v_\theta}{r} \right) + \frac{1}{r^2} \frac{\partial u_r}{\partial \theta} \frac{\partial v_r}{\partial \theta} \right) \\ & + d_{66} \left(\frac{1}{r} \frac{\partial u_\theta}{\partial z} \frac{\partial v_z}{\partial \theta} + \frac{1}{r} \frac{\partial v_\theta}{\partial z} \frac{\partial u_z}{\partial \theta} + \frac{1}{r^2} \frac{\partial u_z}{\partial \theta} \frac{\partial v_z}{\partial \theta} + \frac{\partial u_\theta}{\partial z} \frac{\partial v_\theta}{\partial z} \right) \Bigg\} d\Omega, \end{aligned}$$

and linear functional

$$\langle l, \mathbf{v} \rangle = \int\limits_{\Gamma_N} (\xi_r v_r + \zeta_z v_z + \zeta_\theta v_\theta) d\Gamma.$$

Since axisymmetric objects are considered, we will present the components of the vectors of the surface load in the form of an infinite Fourier series for an angular coordinate

$$\zeta_r = \sum_{i=0}^{\infty} p_r^{(i)} \phi_i(\theta), \quad \zeta_z = \sum_{i=0}^{\infty} p_z^{(i)} \phi_i(\theta), \quad \zeta_\theta = \sum_{i=0}^{\infty} p_\theta^{(i)} \tilde{\phi}_i(\theta). \tag{9}$$

Then the solution of the problem (8) will be found in the form

$$\mathbf{u} = \begin{pmatrix} u_r \\ u_z \\ u_\theta \end{pmatrix} = \sum_{i=0}^{\infty} \left(u_r^{(i)}(r,z,t), u_z^{(i)}(r,z,t), u_\theta^{(i)}(r,z,t), \right) \begin{pmatrix} \phi_i(\theta) & 0 & 0 \\ 0 & \phi_i(\theta) & 0 \\ 0 & 0 & \tilde{\phi}_i(\theta) \end{pmatrix}, \tag{10}$$

where the following notation is introduced

$$\phi_i(\theta) = \{1, \cos\theta, \sin\theta, \cos 2\theta, \sin 2\theta, \ldots, \cos n\theta, \sin n\theta, \ldots\},$$
$$\tilde{\phi}_i(\theta) = \{1, \sin\theta, \cos\theta, \sin 2\theta, \cos 2\theta, \ldots, \sin n\theta, \cos n\theta, \ldots\}$$

– complete orthogonal systems of trigonometric functions on the interval $[0; 2\pi]$.

Partial sum

$$\mathbf{u}_n = \sum_{i=0}^{n} \mathbf{u}^{(i)}(r,z,t) \Phi_i(\theta) \tag{11}$$

is named as the approximation of the weak solution of the problem (8).

Let us select in the subspace of the approximations V_h a basis of piecewise continuous test functions constructed on a regular partition of serendipity quadrilaterals:

$$V_h = span\{N_1, N_2, N_3, \ldots, N_L\}.$$

Then Galerkin's semidiscretization $\mathbf{u}_h^{(i)}(t) \in V_h$ of the weak solution (11) is presented in the form

$$\mathbf{u}_h^{(i)}(r,z,t) = \sum_{k=1}^{L} u_{kh}^{(i)}(t) N_k(r,z) \tag{12}$$

with unknown coefficients $u_{kh}^{(i)}(t)$, which are functions of time. We find these coefficients for one harmonic from the Cauchy problem for a system of ordinary differential equations, which can be presented in matrix notation as

$$\mathbf{M}^{(i)}\ddot{\mathbf{U}}^{(i)}(t)+\mathbf{K}^{(i)}\mathbf{U}^{(i)}(t)=\mathbf{R}^{(i)}(t),\quad \mathbf{U}^{(i)}(0)=\mathbf{0},\quad \dot{\mathbf{U}}^{(i)}(0)=\mathbf{0}. \tag{13}$$

The matrices of mass $\mathbf{M}^{(i)}$ and stiffness $\mathbf{K}^{(i)}$ have the structure

$$\mathbf{M}^{(i)}=\begin{pmatrix} C_1^{(i)}M_{kj}^1+C_6^{(i)}M_{kj}^2 & 0 & 0\\ 0 & C_1^{(i)}M_{kj}^1+C_6^{(i)}M_{kj}^2 & 0\\ 0 & 0 & C_1^{(i)}M_{kj}^1+C_6^{(i)}M_{kj}^2 \end{pmatrix},$$

$$\mathbf{K}^{(i)}=\begin{pmatrix} C_1^{(i)}K_{kj}^{11}+C_2^{(i)}\tilde{K}_{kj}^{11} & C_1^{(i)}K_{kj}^{12} & C_3^{(i)}K_{kj}^{13}+C_4^{(i)}\tilde{K}_{kj}^{13}\\ C_1^{(i)}A_{kj}^{21} & C_1^{(i)}\tilde{K}_{kj}^{22}+C_2^{(i)}\tilde{K}_{kj}^{22} & C_3^{(i)}K_{kj}^{23}+C_4^{(i)}\tilde{K}_{kj}^{23}\\ C_3^{(i)}K_{kj}^{31}+C_4^{(i)}\tilde{K}_{kj}^{31} & C_3^{(i)}K_{kj}^{32}+C_4^{(i)}\tilde{K}_{kj}^{32} & C_5^{(i)}K_{kj}^{33}+C_6^{(i)}\tilde{K}_{kj}^{33} \end{pmatrix},$$
$$k,j=1,2,\ldots,L,$$

and vector of load $\mathbf{R}^{(i)}(t)$

$$\mathbf{R}^{(i)}(t)=\begin{pmatrix} C_1^{(i)}R_k^1(t)\\ C_1^{(i)}R_k^2(t)\\ C_6^{(i)}R_k^3(t) \end{pmatrix},\qquad k=1,2,\ldots,L,$$

with the coefficients

$$R_k^1(t)=\int\limits_{\Gamma_\sigma^1}\zeta_r^{(i)}(t)N_k d\Gamma_\sigma^1,\quad R_k^2(t)=\int\limits_{\Gamma_\sigma^1}\zeta_z^{(i)}(t)N_k d\Gamma_\sigma^1,\quad R_k^3(t)=\int\limits_{\Gamma_\sigma^1}\zeta_\theta^{(i)}(t)N_k d\Gamma_\sigma^1.$$

Here the elements $C_l^{(i)}$, $l=1,\ldots,6$, are the integrals of trigonometric functions.

3.3 Finding a Non-stationary Solution

The solution of problem (13) can be obtained using standard procedures for the solution of the Cauchy problem for ordinary second-order differential equations with constant coefficients. In direct integration, the solution of the system (13) is obtained by a numerical stepwise procedure. The number of operations in this case is directly proportional to the number of steps per time. For integration in time we use the method of expansion according to eigenfunctions.

The nodal values $\mathbf{U}^{(i)}(t)$ of displacement were written as

$$\mathbf{U}^{(i)}(t) = \mathbf{\Psi}_i \mathbf{X}_i(t), \tag{14}$$

where $\mathbf{X}_i(t)$—an unknown vector whose components are generalized displacements, and $\mathbf{\Psi}_i$—the matrix whose columns are eigenvectors obtained as solutions of a generalized algebraic eigenproblem

$$\mathbf{K}^{(i)}\boldsymbol{\psi} = \omega^2 \mathbf{M}^{(i)}\boldsymbol{\psi}, \tag{15}$$

Let us consider that in the time coordinate the solution of variational Eq. (8), can be presented as

$$\mathbf{u} = \mathbf{U}\exp(i\omega t). \tag{16}$$

If we denote $\mathbf{u} = (u_r, u_\theta, u_z)^T$, the amplitude of displacements $\mathbf{u} = \mathbf{U}$, then we obtain the variational equation for $l(t) \equiv 0$

$$a(\mathbf{u},\mathbf{v}) - \omega^2 m(\mathbf{u},\mathbf{v}) = 0, \quad \forall \mathbf{v} \in V.$$

Here the bilinear forms have the form $a(\mathbf{u},\mathbf{v})$, $m(\mathbf{u},\mathbf{v})$ as above.

Let us formulate the following variational problem [6]:

Find a pair $(\mathbf{u},\omega) \in V \times \mathbf{R}$ that

$$a(\mathbf{u},\mathbf{v}) = \omega^2 m(\mathbf{u},\mathbf{v}), \quad \forall \mathbf{v} \in V. \tag{17}$$

Problem (17) is a variational problem of finding eigenvalues $v = \sqrt{\omega/2\pi}$ and their corresponding eigenfunctions. Applying the same approximation as for problem (8), the solution of (17) is reduced to the solution of (15).

Substituting (14) into equations and initial conditions (13) and multiplying to the left at $\mathbf{\Psi}_i^T$, we obtain a system of equilibrium equations for generalized displacements:

$$\ddot{\mathbf{X}}_i(t) + \mathbf{\Omega}_i^2 \mathbf{X}_\mathbf{i}(t) = \mathbf{\Psi}_\mathbf{i}^\mathbf{T} \mathbf{R}^{(i)}(t), \tag{18}$$

with initial conditions $\mathbf{X_i(0)} = \mathbf{0}, \quad \dot{\mathbf{X}}_\mathbf{i}(\mathbf{0}) = \mathbf{0}$.

The system (18) splits into $\tilde{k}$ separate equations

$$\ddot{x}_i^j(\tau) + \left(\omega_i^j\right)^2 x_i^j(\tau) = (\boldsymbol{\psi}_i^j)^T \mathbf{R}^{(i)}(\tau), \quad j = 1,\ldots,\tilde{k}. \tag{19}$$

The solution of each Eq. (19) is represented in the form of the Duhamel integral:

$$x_i^j(t) = \frac{1}{\omega_i^j}\int_0^t (\boldsymbol{\psi}_i^j)^T \mathbf{R}^{(i)}(\xi)\sin\omega_i^j(t-\xi)d\xi + \alpha_i^j \sin\omega_i^j t + \beta_i^j \cos\omega_i^j t. \tag{20}$$

To obtain a complete system response, it is necessary to find a solution of all $\tilde{k}$ Eq. (19). We find the displacements of node points for i—harmonic as a superposition of the reactions of the system in all its eigenvectors.

$$\mathbf{U}^{(i)}(t) = \sum_{k=1}^{\tilde{k}} \mathbf{\Psi}_i^k \mathbf{x}_i^k(t).$$

Finally, the solution is obtained as a linear superposition according to (11) for each Fourier component present in the load.

4 Results

The approbation of the proposed approach with the parallelization was carried out on the cluster of Ivan Franko National University of Lviv, which consists of 14 computing nodes and a server under the Scientific Linux 6.2 (core 3.6.6) operating system. All computing nodes for sharing data between parallel processes are united by 1Gbit/s Ethernet. The problem of determining the dynamic reaction of a hollow cylinder, with internal radii $R_1 = 0.8$ m and external radii $R_2 = 1.2$ m and height $L = 10$ m, with a rigidly pinched lower end was solved. On the outside of the cylinder a non-axisymmetric, non-stationary, normal load is given

$$\tilde{\Psi}(\theta, t) = \begin{cases} \Psi(t)\cos\theta, & -\pi/2 \le \theta \le \pi/2 \\ 0, & |\theta| > \pi/2 \end{cases}, \quad \Psi(t) = 1, \quad \text{for} \quad 0 \le t < \infty.$$

Since the applied load is symmetric with respect to the cross section $\theta = 0$, then only the coefficients with cosines are not nonzero in the expansion in a series of trigonometric functions. They are given by formulas

$$a_0 = 1/\pi, \quad \mathrm{a}_1 = 0.5, \quad \mathrm{a}_n = -\frac{2(-1)^{n/2}}{\pi(n^2-1)}, \quad n = 2, 4, 6, \ldots$$

The physical characteristics of the cylinder were chosen as follows: the density $\rho = 2.7 \times 10^3$ kg/m^3, Poisson's coefficient $\nu = 0.17$ and Young's modulus $E = 0.146 \times 10^{11}$ N/m^2.

The first step for the solution of the dynamic elasticity problem is to find eigenvalues and eigenvectors of free oscillations of the object. Table 1 shows the values of the first five cyclic frequencies of free cylinder oscillations for the first five harmonics, including the zero harmonic. Here i—the column corresponds to i—the harmonic, and j—the row is j—free frequency. It is seen in Table 1 that the smallest free frequency of a cylinder corresponds to the first harmonic. This fact demonstrates that in the study of the dynamic characteristics of cylindrical objects, it is not enough to take into account only symmetric frequencies and their corresponding forms of free vibration.

Table 1. The five cyclic frequencies of free oscillations of the cylinder.

Frequencies	Harmonics				
	0	1	2	3	4
1	38.004	8.864	109.552	490.019	950.804
2	58.204	43.235	115.618	494.395	954.259
3	114.012	96.902	131.759	503.157	960.841
4	190.022	152.402	160.195	516.582	970.737
5	266.043	206.454	198.751	534.887	983.972

There are graphs of the component of the displacement vector by the angular coordinate at the time (t = 0.17 s) on Fig. 1, that corresponds to the largest value of the amplitude of the oscillations. The graphs are marked with: solid line—displacement u_r, dashed line—displacement u_z and dotted-dotted—displacement u_θ. In the section $\theta = 0$ the components u_r, u_z of displacement, and in the section $\theta = \pi/2$ the displacement u_θ take the maximum value.

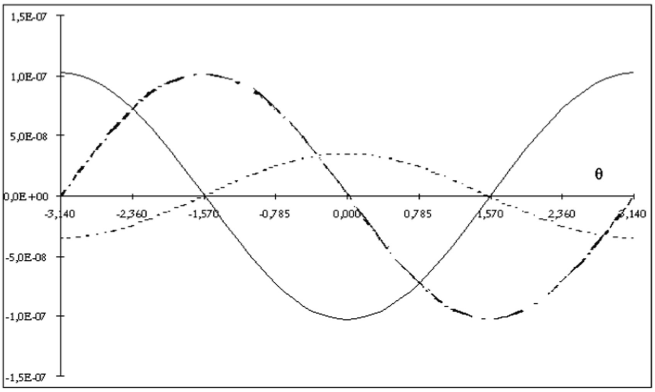

Fig. 1. The values of displacements u_r, u_z, u_θ by angular coordinates θ (rad).

Figure 2 presents graphs of stress changes $\sigma_{\theta\theta}, \sigma_{r\theta}, \sigma_{zz}$ by angular coordinates at the moments of time when the stresses exceed the maximum of the amplitude. The solid, dashed and dotted-dashed lines represent the stresses $\sigma_{\theta\theta}, \sigma_{r\theta}, \sigma_{zz}$, respectively.

5 Conclusion

The numerical investigation of dynamic problems for anisotropic axisymmetric objects within the framework of 3D linear elasticity theory has been developed. Two kinds of dynamic problems have been considered: dynamic response of a structure under an arbitrary load and free vibrations. Semidiscrete FEM with trigonometric series for an angular coordinate is used. The possibility of obtaining asymmetric oscillation frequencies in this scheme is very important. The results of numerical solutions of

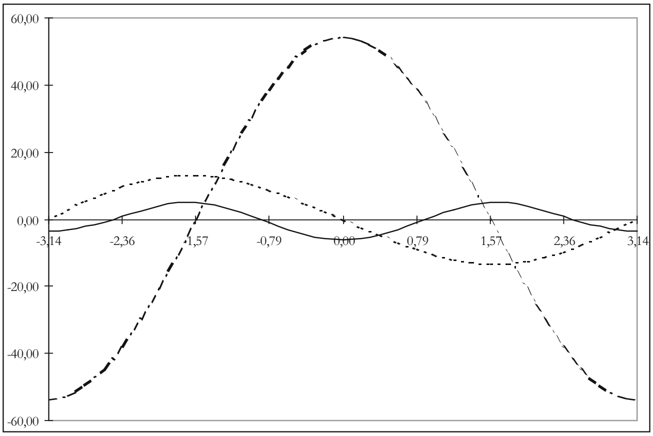

Fig. 2. The values of stresses $\sigma_{\theta\theta}, \sigma_{r\theta}, \sigma_{zz}$ by angular coordinates θ (rad).

engineering problems confirm the effectiveness of the proposed approach. The algorithm of parallel implementation provided the opportunity to significantly reduce the time of obtaining the solution.

References

1. Khimich, A., Popov, A., Chistyakov, O.: Hybrid algorithms for solving the algebraic eigenalue problem with sparse matrix. Cybern. Syst. Anal. **53**(6), 132–146 (2017)
2. Sun, Q., Klaseboer, E., Khoo, B., Chan, D.: Boundary regularized integral equation formulation of the Helmholtz equation in acoustics. R. Soc. Open Sci. **2**, 140520 (2015)
3. Cui, X.Y., Li, G.Y.: An explicit smoothed finite element method (SFEM) for elastic dynamic problems. Int. J. Comput. Methods **10**(1) (2013)
4. Kosloff, D., Kesslerz, D., Filho, A.Q., Tessmer, E., Behle, A., Strahilevitz, R.: Solution of the equations of dynamic elasticity by a Chebychev spectral method. Geophysics **55**(6), 734–748 (1990)
5. Hasheminejada, S., Mirzaei, Y.: Three dimensional vibration analysis of a class of traction-free solid elastic bodies with an eccentric cavity. Shock Vibr. **19**, 1341–1357 (2012)
6. Grigorenko, A., Dyyak, I., Makar, V.: Influence of anisotropy on the response characteristics of finite cylinders under free vibrations. Int. Appl. Mech. **37**(5), 628–637 (2001)
7. Dong, S., Yosibash, Z.: A parallel spectral element method for dynamic three-dimensional nonlinear elasticity problems. Comput. Struct. **87**, 59–72 (2009)
8. Dyyak, I., Prokopyshyn, I., Martynyak, R.M., Prokopyshyn, I.A.: Domain decomposition methods for problems of unilateral contact between elastic bodies with non-linear winkler covers. In: Erhel, J., Gander, M.J., oth (eds.) Lecture Notes in Computational Science and Engineering, pp. 739–748. Springer International Publishing, Switzerland (2014)
9. Bardzokas, D., Kushnir, D., Filshtinskii, L.: Dynamic problems of the theory of elasticity for layers and semilayers with cavities. Acta Mech. **208**, 81–95 (2009)
10. Hager, C., Wohlmuth, B.I.: Analysis of a space-time discretization for dynamic elasticity problems based on mass-free surface elements. SIAM J. Numer. Anal. **47**(3), 1863–1885 (2009)